Computational Studies of Gas-Phase Ca_3P_2 and Ca_6P_4

Chammi S. Palehepitiya Gamage, Kaori Ueno-Noto, and Dennis S. Marynick*

Department of Chemistry and Biochemistry, University of Texas at Arlington, Arlington, Texas 76019-0065

Received: May 30, 2009; Revised Manuscript Received: July 16, 2009

The electronic and molecular structures of Ca_3P_2 and Ca_6P_4 are investigated using high-level ab initio methods. The lowest energy structure for Ca_3P_2 is found to be a Jahn−Teller distorted triplet. An excited-state singlet is found with various post HF methods; however, DFT incorrectly predicts a closed shell singlet to be the ground state. For the Ca_6P_4 system, both DFT and ab initio methods give consistent relative energies. The computational results demonstrate that the energetics are very sensitive to the size of the Ca basis set. Enhancing the Ca basis sets with additional s and p valence functions significantly affects the calculated energies.

Introduction

Compounds containing alkaline earth metals and group V elements are of interest for a variety of reasons. These compounds are generally referred to as pnictides.[1,2] Mg_3N_2 and Ca_3N_2 are well-known as nontoxic semiconducting pigments and are also thermoelectric materials.[3−10] Bulk Ca_3P_2 and Ca_3As_2 are also widely used in commercial applications.[11,12]

To date, theoretical studies on these systems have been mainly limited to studies of the nature of the solid-state electronic structure. To our knowledge, there are no electronic or molecular structure studies, experimental or theoretical, for individual molecules or small clusters of these systems in the literature. In this article, we extend our previous work on the relationship between the molecular and solid-state structures of simple main group systems such as $(AgBr)_n$,[13] $(PbS)_n$,[14] and $(CdS)_n$[15] by exploring the molecular and electronic structures of Ca_3P_2 and Ca_6P_4. We identify two energetically competitive electronic states for Ca_3P_2 and find that the ground state can be thought of as a Jahn−Teller distorted triplet. We also report the calculated molecular structures for various Ca_6P_4 clusters.

Computational Details

All calculations were performed using the Gaussian 03 suite of programs.[16] To locate multiple local minima on the potential energy surface, many possible starting geometries were considered. Initial geometries were obtained at the HF/Ca: 3-21G, P: 3-21+G level. Final geometries were calculated using a hybrid basis set as follows: we modified the Gaussian basis set 6-311G* for Ca[17−19] and utilized the Gaussian basis set 6-311+G* for P.[19] The Ca basis set was enhanced by decontracting the valence d function from 3/1 to 2/1/1 (denoted 6-311G*′). This basis set combination was found to yield reasonable results and was less computationally demanding for these systems when testing against several combinations of different basis sets. These structures were then reoptimized at the HF, MP2, MP4, CISD, CCSD, QCISD, and DFT levels (B3LYP functional) using the above-mentioned hybrid basis set.[20−22] The core orbitals in the MP2, MP4, CCSD, and QCISD calculations were assigned according to G2 convention (i.e., only the 1s, 2s, and 2p orbitals were frozen). Additional basis set combinations such as I Ca: 6-311G*′, P: 6-311+G*, II Ca: 6-311G*′, P: 6-31+G*, III Ca: 6-31G*, P: 6-311+G*, IV Ca: 6-311G*″, P: 6-311+G*, V Ca: cc-PVTZ, P: 6-311+G* were used to verify the accuracy of the above basis set using the MP2 method for the Ca_3P_2 system. The basis set 6-311G*″ was constructed by expanding the valence functions of the 6-311G*′ basis set from (14s, 11p, 4d) to (17s, 14p, 4d). The additional s and p exponents were optimized for the CaS system at the MP2 level using the gauopt utility.[23] In addition, single-point energy calculations were performed for all the optimized geometries using the MP4, CCSD, CCSD(T), QCISD, and QCISD(T) methods with Ca: 6-311G*′ and P: 6-311+G*.[20−22] Wave function stability was tested for all ground-state geometries when possible. Analytical frequency calculations were performed when available, and geometries that did not correspond to a minimum were distorted along the imaginary frequency and reoptimized until a true minimum was found. Natural bond orbital (NBO) analysis was performed for the Ca_3P_2 system using the CCSD density.[24]

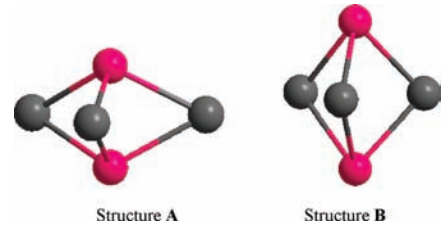

Figure 1. Lowest energy structures of Ca_3P_2 at the MP2/Ca: 6-311G*′ P: 6-311+G* level.

Results and Discussion

Structures of the Ca_3P_2 System. Figure 1 illustrates the lowest energy structures found for Ca_3P_2. Structure A is a triplet, and structure B is a singlet. The lowest energy structure at all levels except DFT (see below) is A. Structure A has C_{2v} symmetry and may be viewed as a distorted trigonal prism, while structure B possesses exact D_{3h} symmetry (Tables 1 and 2). Structure A was obtained by initially optimizing to a triplet D_{3h} geometry, which was unstable at the HF level. Breaking the symmetry then resulted in a minimum with a stable wave function and C_{2v} symmetry.

Descriptive Electronic Structures of the Ca_3P_2 System. To understand the electronic structures of these systems, NBO analysis was performed at the CCSD level. The analysis shows

* To whom correspondence should be addressed. E-mail: dennis@uta.edu.

10.1021/jp9050935 CCC: $40.75
Published on Web 08/13/2009

TABLE 1: Relative Energies of Structures A and B after Geometry Optimization Using Different Levels of Electron Correlation and the Ca: 6-311G*′ P: 6-311+G* Basis Sets (ΔE Is the Relative Energy of the Two Species with the Energy of the Triplet Taken as 0.0)

method	ΔE (kJ/mol)	system	P−P distance (Å)	point group
HF	0.0	triplet	2.450	C_{2v}
	117.2	singlet	3.959	D_{3h}
MP2	0.0	triplet	2.500	C_{2v}
	28.3	singlet	3.916	D_{3h}
MP4	0.0	triplet	2.500	C_{2v}
	40.5	singlet	3.956	D_{3h}
CISD	0.0	triplet	2.448	C_{2v}
	55.2	singlet	3.991	D_{3h}
CCSD	0.0	triplet	2.511	C_{2v}
	44.0	singlet	3.958	D_{3h}
QCISD	0.0	triplet	2.514	C_{2v}
	37.2	singlet	3.968	D_{3h}
B3LYP	0.0	triplet	2.481	C_{2v}
	−18.1	singlet	3.865	D_{3h}

TABLE 2: Bond Lengths and Angles for the Ca_3P_2 Systems from the MP2 Optimized Structures

system	P−P (Å)	Ca−P (Å)	Ca−Ca (Å)	Ca−P−Ca (deg)	P−Ca−P (deg)
structure A	2.500	2.763	4.036	97.51	53.80
		2.603	4.414	106.02	57.38
structure B	3.916	2.789	3.317	74.53	91.26

TABLE 3: [13]NBO Analysis for the Ca_3P_2 Triplet-State Structure[a]

orbital Ca_3P_2	occupancy		%	hybrid (%) s	p	d
Triplet	Alpha					
BD(Ca−P)	0.7	Ca	10.64	0.68	93.65	5.73
		P	89.36	8.11	91.89	
BD(Ca−P)	0.768	Ca	50.00	96.9	3.02	0.08
		Ca	50.00	96.9	3.02	0.08
LP(P)	0.979			94.8	5.2	
LP(P)	0.919			1.4	98.6	
LP(P)	0.911			0	100	
LP(P)	0.64			6.35	93.65	
LP(P)	0.979			94.79	5.21	
LP(P)	0.919			1.42	98.58	
LP(P)	0.911			0	100	
	Beta					
BD(P−P)	0.956	P	50.00	4.4	95.6	
		P	50.00	4.4	95.6	
LP(P)	0.944			87.96	12.04	
LP(P)	0.935			0	100	
LP(P)	0.933			7.73	92.27	
LP(P)	0.944			87.96	12.04	
LP(P)	0.935			0	100	
LP(P)	0.933			7.73	92.27	
Atom	Natural Charges					
Ca	0.886					
Ca	0.908					
Ca	0.908					
P	−0.851					
P	−0.851					

[a] BD = two-center bond; LP = lone pair.

that the triplet-state molecule is quite ionic (Table 3). There is a P−P bond (with a calculated distance of 2.50 Å, compared to 2.23 Å for the P−P bond in P_2H_2 at the MP2/6-31G** level).[25] Taking the pseudo threefold axis as y, each P atom has a pure 3s lone pair and two lone pairs derived from p_x and p_z. The P−P bond is formed by overlap of the p_y orbitals. The driving force for the formation of the triplet is the formation of the P−P bond. The electrons from the lone pairs and the bonding electrons complete the octet around each P atom. The remaining two electrons reside on Ca orbitals and are most easily described in the symmetry basis. One electron occupies a Ca−Ca pseudo a′ bonding orbital in D_{3h} symmetry. The remaining electron could also occupy the same a′ bonding orbital, or it could occupy one of the two pseudo e″ orbitals, leading to a Jahn−Teller distortion. The latter configuration turns out to be the ground state. The NBO analysis yields a schematic representation of the resonance structures for the triplet-state structure as summarized in Figure 2. The details of the NBO results are shown in Table 3.

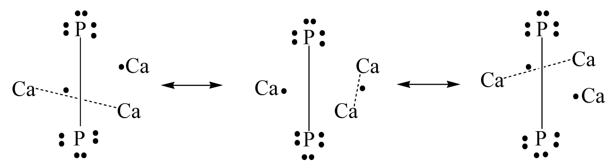

Figure 2. Schematic electronic resonance structures for the triplet state of Ca_3P_2 derived from an NBO analysis at the CCSD level.

TABLE 4: NBO Analysis for the Ca_3P_2 Singlet-State Structure[a]

orbital Ca_3P_2	occupancy		%	hybrid (%) s	p	d
Singlet						
BD(Ca−P)	1.853	Ca	8.00	48.82	9.36	41.81
		P	92.00	4.11	95.66	0.23
BD(Ca−P)	1.909	Ca	8.00	48.82	9.36	41.81
		P	92.00	4.11	95.66	0.23
BD(Ca−P)	1.909	Ca	8.00	48.82	9.36	41.81
		P	92.00	4.11	95.66	0.23
BD(Ca−P)	1.909	Ca	8.00	48.82	9.36	41.81
		P	92.00	4.11	95.66	0.23
BD(Ca−P)	1.909	Ca	8.00	48.82	9.36	41.81
		P	92.00	4.11	95.66	0.23
BD(Ca−P)	1.909	Ca	8.00	48.82	9.36	41.81
		P	92.00	4.11	95.66	0.23
LP(P)	1.947			88.07	11.91	0.02
LP(P)	1.947			88.07	11.91	0.02
Atom	Natural Charges					
Ca	1.462					
Ca	1.462					
Ca	1.462					
P	−2.193					
P	−2.193					

[a] BD = two-center bond; LP = lone pair.

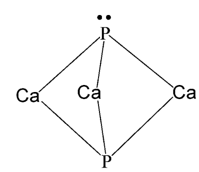

Figure 3. Summary of the NBO results for the singlet state of Ca_3P_2.

The NBO analysis of the electronic structure of the singlet-state structure is straightforward. Each P atom has a single 3s lone pair and three Ca−P bonds. The details of the NBO results are shown in Table 4. The structure has perfect trigonal bypyramidal geometry and a long P−P distance, consistent with the absence of a P−P bond. Figure 3 summarizes the NBO results for the singlet.

Energy Discrepancy at Different Levels of Theory. As shown in the Table 1, the relative energies (ΔE is defined as

TABLE 5: Relative Energies Calculated Using Different Levels of Electron Correlation[a]

method	ΔE (kJ/mol)
HF	117.2
MP2	28.3
MP3	53.5
MP4	40.5
CISD	55.2
QCISD	37.2
QCISD(T)	34.1
CCSD	44.0
CCSD(T)	37.7
B3LYP	–19.2
BLYP	–35.4
BP86	–31.2
B3P86	–20.0

[a] Method/(Ca: 6-311G*′, P: 6-311+G*)//MP2/(Ca: 6-311G*′, P: 6-311+G*) ($\Delta E = E_{SINGLET} - E_{TRIPLET}$).

TABLE 6: Relative Energies Calculated Using Various Basis Set Combinations at the CCSD Level ($\Delta E = E_{SINGLET} - E_{TRIPLET}$)

basis set	ΔE (kJ/mol)
1. Ca: 6-311G*′, P: 6-311+G*	55.2
2. Ca: 6-311G*′, P: 6-31+G*	54.2
3. Ca: 6-311G*′, P: 6-311+G(2d)	16.1
4. Ca: 6-311G*′, P: 6-311+G(2df)	22.5
5. Ca: 6-31G*, P: 6-311+G*	83.4
6. Ca: 6-311G*″, P:6-311+G*	20.9
7. Ca: cc-PVTZ′,[a] P: 6-311+G*	13.2

[a] cc-PVTZ basis set was used without f functions.

$E_{SINGLET} - E_{TRIPLET}$) for the singlet and triplet are significantly different, especially at the HF and DFT levels (117.2 and −18.1 kJ/mol are clear outliers). Both structures were fully geometry optimized at the HF, MP2, MP4, CISD, CCSD, QCISD, and DFT levels to evaluate energies. All HF and post-HF methods predict that the triplet is the ground state. However, at the DFT level, the singlet state was identified as the lowest energy structure, 18.1 kJ/mol lower energy than the triplet. However, the optimized geometries at all levels are similar. Table 2 shows the optimized geometries at the MP2 level.

To understand this discrepancy, while eliminating effects due to variations in optimized geometries at different levels, all energetic were recalculated using the same MP2 optimized geometries (Table 5) with Ca: 6-311G*″, P: 6-311+G*. The calculated energy differences remained consistent with the energies of the fully geometry optimized structures, and all non-DFT methods predicted the triplet to be the ground state, with ΔE's in the range ∼28−55 kJ/mol. Higher degrees of electron correlation tend to lower the energy difference between the two species. However, the DFT (B3LYP) approach predicts the singlet to be ∼19 kJ/mol more stable that the triplet. Given that high-level ab initio methods such as CCSD(T) should be significantly more accurate than DFT, it seems very likely that DFT makes an erroneous prediction for the ground state of this species. As seen in Table 5, other commonly used DFT functionals yield results similar to that of B3LYP.

Sensitivity of the System to Size of the Ca Basis Set. We checked the sensitivity of the system to different basis set selections. All calculations were performed at the CCSD level with different basis set combinations using the MP2 optimized geometries. As indicated in the first four lines of Table 6, increasing the size of the phosphorus basis set generally lowers the calculated ΔE. However, increasing the Ca basis set size has a much greater effect. The small basis set 6-31G* gives a relative energy much higher than that calculated with the larger basis sets. Our results suggest that the choice of Ca basis set is crucial to the calculation of reliable energetic and that small to medium size standard Ca basis sets commonly found in the literature should be used with caution.

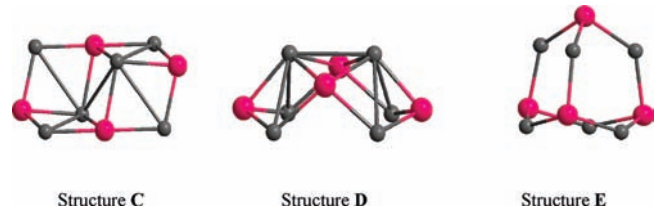

Figure 4. Lowest energy structures of Ca_6P_4 at the MP2/Ca: 6-311G*′ P: 6-311+G* level.

TABLE 7: Relative Energies of the Different Geometries of Ca_6P_4 (Energy of Structure C Is Taken as 0.0)

	ΔE (kJ/mol)	
structure	MP2	B3LYP
structure C	0.0	0.0
structure D	59.2	62.8
structure E	85.8	75.7

TABLE 8: Single-Point Energy Calculation with Various Methods Using Method/Ca: 6-311G*, P: 6-311+G*//MP2/Ca: 6-311G*, P: 6-311+G* (Energy of Structure C Is Taken as 0.0)

	ΔE (kJ/mol)	
structure	CCSD	QCISD
structure C	0.0	0.0
structure D	60.6	60.2
structure E	74.1	75.8

Ca_6P_4 System. For the Ca_6P_4 system, three structures were found as minimum energy candidates as shown in Figure 4. The relative energies of the fully geometry optimized structures were obtained using MP2 (DFT results are also shown for comparison in Table 7). More interestingly, for the dimer system, the post HF methods and DFT gave consistent relative energies, unlike the Ca_3P_2 system. All structures were tested for stability, and it was found that, for all three structures, the singlet-state wave functions were stable. The single-point energies of these systems were also calculated using higher levels of theory such as CCSD and QCISD and the larger basis sets Ca: 6-311G*′ and P: 6-311+G* (Table 8). The relative energies obtained at the CCSD and QCISD levels are consistent with both MP2 and DFT results. This is not surprising, given that the dimers are more coordinatively saturated, with larger HOMO−LUMO gaps and thus fewer low-lying excited states. This phenomena has been discussed in detail in our previous work on AgBr clusters.[13]

Structure C was found to be lowest in energy (the bond distances and angles are listed in Table 9). This structure has C_{2h} symmetry. Structure D is a boat-shaped molecule with C_{2v} symmetry. Structure E has a relatively high energy. The formation of the dimer from the ground-state monomer

$$2Ca_3P_2 \rightarrow Ca_6P_4$$

is very exothermic: −536.1 kJ/mol at the MP2/Ca: 6-311G*′ P: 6-311+G* level.

TABLE 9: Bond Lengths and Angles for Optimized Geometries Using the MP2 Method

system	P−P (Å)	Ca−P (Å)
structure C	3.432	2.655
	3.435	2.803
	3.517	2.833
structure D	3.335	2.665
	3.438	2.731
		2.765
		2.840
structure E		2.686

Summary

In this study, we computed electronic and molecular structures for the Ca_3P_2 and Ca_6P_4 systems using high-level ab initio methods. For Ca_3P_2, we found two minimum energy structures: the minimum is a triplet-state Jahn−Teller distorted structure with C_{2v} symmetry and the other one is a singlet-state structure with D_{3h} symmetry. Ca_3P_2 is sensitive to the level of the theory applied, especially the quality of the Ca basis set and the methodology for electron correlation (post HF or DFT). Particularly noteworthy is the failure of DFT to predict the correct ground-state multiplicity for Ca_3P_2. Three structures were found for the $[Ca_6P_4]$ system, and they were all singlet state. Ab initio and DFT methods yielded consistent results for the dimer.

Acknowledgment. This work was supported by a grant from the Welch Foundation to D.S.M. (Grant Y-0743).

References and Notes

(1) Imai, Y.; Watanabe, A. *J. Mater. Sci.* **2006**, *41*, 2435.
(2) Xu, R.; de Groot, R. A.; van der Lugt, W. *J. Phys.: Condens. Matter* **1993**, *5*, 7551.
(3) Fang, C. M.; De Groot, R. A.; Bruls, R. J.; Hintzen, H. T.; De With, G. *J. Phys.: Condens. Matter* **1999**, *11*, 4833.
(4) Mokhtari, A.; Akbarzadeh, H. *Physica B* **2003**, *337*, 122.
(5) Heyns, A. M.; Prinsloo, L. C.; Range, K.-J.; Stassen, M. *J. Solid State Chem.* **1998**, *137*, 33.
(6) Orhan, E.; Jobic, S.; Brec, R.; Marchand, R.; Saillard, J. Y. *J. Mater. Chem.* **2002**, *12*, 2475.
(7) Laurent, Y.; Lang, J.; Le Bihan, M. T. *Acta Crystallogr., Sect. B* **1968**, *24*, 494.
(8) Partin, D. E.; Williams, D. J.; O'Keeffe, M. *J. Solid State Chem.* **1997**, *132*, 56.
(9) Watson, L. M.; Marshall, C. A. W.; Cardoso, C. P. *J. Phys. F: Met. Phys.* **1984**, *14*, 113.
(10) Vansant, P. R.; Van Camp, P. E.; Van Doren, V. E.; Martins, J. L. *Phys. Rev. B: Condens. Matter* **1998**, *57*, 7615.
(11) Min, D. J.; Sano, N. *Metall. Trans. B* **1989**, *20*, 863.
(12) Paoloni, A. *Fertilizer and Fungicide*; Gotthardwerke AG für Elektrochemische Industrie: Bodio, Switzerland, 1930; pp Addn to 146.
(13) Zhang, H.; Schelly, Z. A.; Marynick, D. S. *J. Phys. Chem. A* **2000**, *104*, 6287.
(14) Zeng, H.; Schelly, Z. A.; Ueno-Noto, K.; Marynick, D. S. *J. Phys. Chem. A* **2005**, *109*, 1616.
(15) Zeng, H.; Vanga, R. R.; Marynick, D. S.; Schelly, Z. A. Submitted for publication.
(16) Frisch, M. J.; Trucks, G. W.; Schlegel, H. B.; Scuseria, G. E.; Robb, M. A.; Cheeseman, J. R.; Montgomery, J. A., Jr.; Vreven, T.; Kudin, K. N.; Burant, J. C.; Millam, J. M.; Iyengar, S. S.; Tomasi, J.; Barone, V.; Mennucci, B.; Cossi, M.; Scalmani, G.; Rega, N.; Petersson, G. A.; Nakatsuji, H.; Hada, M.; Ehara, M.; Toyota, K.; Fukuda, R.; Hasegawa, J.; Ishida, M.; Nakajima, T.; Honda, Y.; Kitao, O.; Nakai, H.; Klene, M.; Li, X.; Knox, J. E.; Hratchian, H. P.; Cross, J. B.; Bakken, V.; Adamo, C.; Jaramillo, J.; Gomperts, R.; Stratmann, R. E.; Yazyev, O.; Austin, A. J.; Cammi, R.; Pomelli, C.; Ochterski, J. W.; Ayala, P. Y.; Morokuma, K.; Voth, G. A.; Salvador, P.; Dannenberg, J. J.; Zakrzewski, V. G.; Dapprich, S.; Daniels, A. D.; Strain, M. C.; Farkas, O.; Malick, D. K.; Rabuck, A. D.; Raghavachari, K.; Foresman, J. B.; Ortiz, J. V.; Cui, Q.; Baboul, A. G.; Clifford, S.; Cioslowski, J.; Stefanov, B. B.; Liu, G.; Liashenko, A.; Piskorz, P.; Komaromi, I.; Martin, R. L.; Fox, D. J.; Keith, T.; Al-Laham, M. A.; Peng, C. Y.; Nanayakkara, A.; Challacombe, M.; Gill, P. M. W.; Johnson, B.; Chen, W.; Wong, M. W.; Gonzalez, C.; Pople, J. A. Gaussian 03, revision C.02; Gaussian, Inc.: Wallingford, CT, 2004.
(17) Rassolov, V. A.; Ratner, M. A.; Pople, J. A.; Redfern, P. C.; Curtiss, L. A. *J. Comput. Chem.* **2001**, *22*, 976.
(18) Blaudeau, J.-P.; McGrath, M. P.; Curtiss, L. A.; Radom, L. *J. Chem. Phys.* **1997**, *107*, 5016.
(19) Extensible Computational Chemistry Environment Basis Set Database, version 02/02/06; Pacific Northwest Laboratory: Richland, WA, 2006.
(20) Leach, A. R. *Molecular Modelling: Principles and Applications*; Prentice Hall: New York, 2001.
(21) Hinchliffe, A. *Computational Quantum Chemistry*; Wiley & Sons: New York, 1988.
(22) Roresman, J. B.; Frisch, A. *Exploring Chemistry with Electronic Structure Methods*; Gaussian, Inc.: Pittsburgh, PA, 1996.
(23) New exponents are for s, 2.12, 0.74, 0.44E-01; for p, 1.32, 1.09, 0.51, 0.39E-01.
(24) Glendening, E. D. R.; Reed, A. E.; Carpenter, J. E.; Weinhold, F. NBO 3.1; Gaussian, Inc.: Wallingford CT, 2004.
(25) Lammertsma, K.; Guner, O. F.; Sudhakar, P. V. *J. Chem. Phys.* **1991**, *94*, 8105.

JP9050935